THE GEOLOGICAL SOCIETY OF AMERICA®

Peak intervals of equatorial Pacific export production during the middle Miocene climate transition

Samantha C. Carter[1], Elizabeth M. Griffith[1], Donald E. Penman[2]
[1]Department of Earth and Environmental Sciences, University of Texas at Arlington, 500 Yates Street, Arlington, Texas 76019, USA
[2]Department of Geology and Geophysics, Yale University, P.O. Box 208109, New Haven, Connecticut 06520, USA

ABSTRACT

The middle Miocene climate transition (MMCT) is characterized by an abrupt 1‰ increase in benthic foraminiferal oxygen isotopes at ca. 13.8 Ma, marking expansion of the Antarctic Ice Sheet and transition of Earth's climate to a cooler, relatively stable glacial state. Also occurring during this period is a globally recognized positive carbon isotope excursion (16.9–13.5 Ma) in benthic and planktonic foraminifera with shorter carbon isotope maxima (CM) events, linking hypotheses for climate change at the time with the carbon cycle. In order to test whether export production in the eastern equatorial Pacific is related to the largest such event (CM6), coincident with Antarctic Ice Sheet expansion, a high-resolution (<5 k.y.) record of export production at Integrated Ocean Drilling Program Site U1337 spanning the MMCT (14.02–13.43 Ma) was produced using marine pelagic barite mass accumulation rates. Export production is elevated with an extended period of more than double present-day values. These variations are not orbitally paced and provide evidence for a reorganization of nutrients supplied to the eastern equatorial Pacific in the Miocene and intensification of upwelling. If such changes are representative of the entire region, then this mechanism could sequester enough carbon to have a significant effect on atmospheric pCO_2. However, continual delivery of nutrients to the surface waters of the eastern equatorial Pacific is required in order to sustain export production without depleting the surface ocean of limiting nutrients. This might be accomplished by a change in ocean circulation or a combination of other processes requiring further study.

INTRODUCTION

The middle Miocene climate transition (MMCT) is one of three major benthic foraminiferal oxygen isotope ($\delta^{18}O$) events during the Cenozoic that reflect key expansions of polar ice sheets on Earth (Zachos et al., 2001). Expansion of the Antarctic Ice Sheet (AIS) occurred toward the end of a globally recognized long positive carbon isotope ($\delta^{13}C$) excursion called the Monterey event, traditionally interpreted as the result of increased burial of organic carbon (C_{org}) around the Pacific Rim (Vincent and Berger, 1985). The Monterey event started during a period of global warmth after 16.9 Ma, and ended at ca. 13.5 Ma, ~400 k.y. after expansion of the AIS. Within this broad $\delta^{13}C$ excursion, a series of short-lived, higher-frequency $\delta^{13}C$ maxima (CM) events have been recognized that exhibit strong ~400 k.y. cyclicity and high coherence with long eccentricity (Holbourn et al., 2007). Each CM event coincides with an increase in $\delta^{18}O$; the largest, CM6, occurred at the same time as the major expansion of the AIS at ca. 13.8 Ma, suggesting a link between the global carbon cycle and ice volume (Woodruff and Savin, 1991; Shevenell et al., 2008).

Atmospheric pCO_2 reconstructions show generally low (~300 ppm) pCO_2 during the warm Miocene world with much less ice than today (Pagani et al., 1999; Kürschner et al., 2008; Foster et al., 2012; Badger et al., 2013). A decrease of ~60–80 ppm associated with CM6 (Badger et al., 2013) supports the hypothesis that increased C_{org} burial drew down atmospheric pCO_2, facilitating ice sheet expansion. However, many questions remain regarding what caused the increase in C_{org} burial, where, when, and if it occurred, and whether it was a feedback within the climate system or caused the MMCT. Some evidence suggests that increased productivity in the marine (Vincent and Berger, 1985; Holbourn et al., 2014) and/or terrestrial (Diester-Haass et al., 2009) environment caused the increase in C_{org} burial. However, it is also possible to increase C_{org} burial by increasing preservation through the expansion of oxygen minimum zones (Woodruff and Savin, 1991) or decreasing ocean temperatures (Lyle and Baldauf, 2015). Alternatively, lowering the $CaCO_3$ to C_{org} rain ratio could decrease atmospheric pCO_2 concentrations without necessarily a change in marine productivity (Sigman and Boyle, 2000; Kender et al., 2014).

Drilling at Integrated Ocean Drilling Program (IODP) Site U1337 (3°50.009′N, 123°12.352′W, 4436 m modern water depth; Fig. 1) recovered a continuous carbonate-rich middle Miocene succession from the eastern equatorial Pacific (EEP), a narrow region with high primary productivity brought on by Ekman-induced upwelling of deep, nutrient-rich waters (Chavez and Barber, 1987). Site U1337 is ideally situated because it remained within the EEP between 24.4 and 8 Ma (Pälike et al., 2010). Today, this region has low biological pump efficiency (i.e., phytoplankton are unable to completely draw down surface nutrient concentrations) and low particle export fraction (Sarmiento and Gruber, 2006), predominantly because primary production is limited by the micronutrient iron (Martin et al., 1994).

High-resolution records from X-ray fluorescence (XRF) scanner-derived elemental data from cores in this region provide some evidence supporting the hypothesis that enhanced marine productivity contributed to atmospheric pCO_2 drawdown just before and during AIS expansion

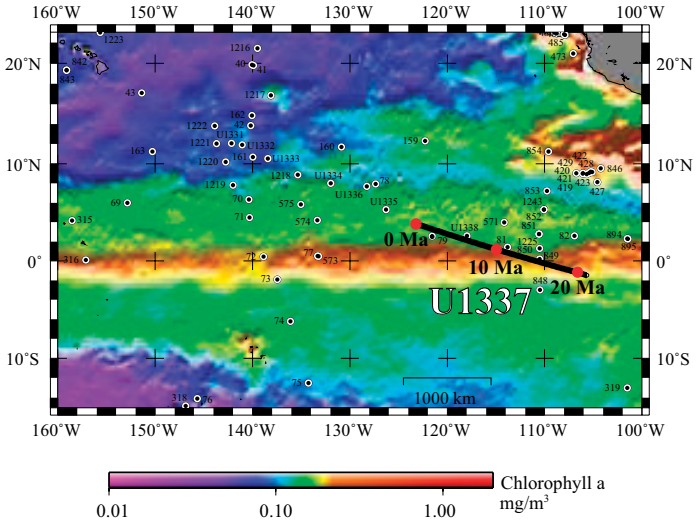

Figure 1. Present-day location of Integrated Ocean Drilling Program Site U1337 with backtracked locations through 20 Ma (modified from Pälike et al., 2010).

Data Repository item 2016310 | doi:10.1130/G38290.1

(Holbourn et al., 2014; Shackford et al., 2014; Lyle and Baldauf, 2015). Quantification of changes in production using the existing records is complicated; however, it is necessary to fully evaluate the role this region played in global carbon cycling during the MMCT.

Our study presents a high-resolution record of export production, the fraction of C_{org} that is removed from the surface ocean and sinks into the deep ocean, from sedimentary marine pelagic barite ($BaSO_4$) accumulation in the EEP to verify and quantify changes. Marine barite is a widely distributed highly refractory minor component of marine sediments formed from decaying organic matter as it sinks through the water column and accumulates beneath areas of high productivity (e.g., Paytan and Griffith, 2007). Barite mass accumulation rates (BAR) have a strong correlation with C_{org} export in core top sediments, allowing for direct calculation of export C (e.g., Paytan et al., 1996; Eagle et al., 2003). Assuming the processes that govern barite precipitation and accumulation in the deep sea have remained constant through time, changes in BAR reflect variations in export production and can be used to quantify changes in the geologic past. Interpreting these new results in combination with changes in $\delta^{18}O$ and $\delta^{13}C$ (Tian et al., 2013) and XRF records (Shackford et al., 2014) from the same core provides insight into the relationship between the carbon cycle, climate change, and global ice volume.

METHODS

A high-resolution record of BAR and $CaCO_3$ mass accumulation rates (CAR) over the MMCT was produced from deep-sea sediment samples collected at IODP Site U1337. Barite was separated from the sediment following a procedure adapted from Paytan et al. (1996) and screened for purity using scanning electron microscopy. The weight percent barite was converted to accumulation rates using a modified age model from Tian et al. (2013) and dry bulk density values estimated by linear interpolation between shipboard measurements (Pälike et al., 2010). Accumulation rates are used to remove variability on longer time scales due to dilution; however, these calculations are only as accurate as the age model from which they are derived. BAR was then converted to export production using the relationship specific to the equatorial Pacific from Eagle et al. (2003). The same samples were analyzed for total inorganic carbon content to calculate CAR (for additional details, see the GSA Data Repository[1]).

ELEVATED EEP EXPORT PRODUCTION OVER THE MMCT

The BAR record from this study gives evidence for large fluctuations in export production over the MMCT in the EEP (Fig. 2). Two peaks in BAR at 13.83 and 13.59 Ma and a period of elevated BAR from 13.99 to 13.92 Ma coincide with drops in CAR and peaks in XRF-derived biogenic silica accumulation from the same site (Shackford et al., 2014; Fig. 2) and nearby Site U1338 (Holbourn et al., 2014). Variations in BAR and biogenic silica accumulation are independent of changes in MAR, while CAR appears to be controlled primarily by MAR (Fig. DR4 in the Data Repository). The calculated rain ratio of $CaCO_3$ to C_{org} (CAR:BAR) changes most notably during intervals of peak BAR (Fig. DR3) and could contribute to pCO_2 drawdown; however, quantification is complicated by potential changes in carbonate preservation and remineralization of organic matter in deep water (Griffith et al., 2010).

Benthic foraminiferal $\delta^{18}O$ and $\delta^{13}C$ records show strong imprints of orbital periodicity, particularly obliquity (~40 k.y.) and eccentricity (100 k.y. and 400 k.y.), consistent with previous records from other sites (Tian et al., 2013). BAR does not exhibit the same periodicity, nor does it show significant coherence with either isotopic record (Figs. DR6 and DR7). This suggests that there is not a simple relationship between export production, changes in $\delta^{18}O$ and $\delta^{13}C$, and insolation. However, our BAR record is not long enough to resolve the long eccentricity cycle of 400 k.y. that is thought to pace long-term carbon cycling during the Miocene (e.g., Woodruff and Savin, 1991). Export production seems to be responding to critical thresholds in Earth's internal climate system, such as nutrient supply via changes in ocean circulation, that could be related to but are not paced by orbital periodicity.

PRECONDITIONING THE CLIMATE SYSTEM

An extended time period of elevated BAR (13.99–13.92 Ma) has an average value of 9.88 mg cm^{-2} $k.y.^{-1}$ corresponding to 103 gC m^{-2} y^{-1} of exported carbon, more than twice present-day values. There is also strong evidence of an increase in biogenic silica production at that time (Holbourn et al., 2014; Shackford et al., 2014), suggesting that this increase in export production is caused by elevated primary productivity by diatoms, as opposed to solely a change in biological pump efficiency. Primary productivity in this region could be increased by intensification of equatorial upwelling and/or a change in the nutrient supply to the region.

Intensification of equatorial upwelling linked to high-latitude cooling, both before and during expansion of the AIS, was suggested as the cause of increased silica production in the EEP (Holbourn et al., 2014). This hypothesis was discounted by Lyle and Baldauf (2015) because of an apparent tenfold increase in silica (and barium) accumulation at that time at Site U1338, which would require too extreme an increase in trade winds to sustain over that time period. However, our new data suggest that the increase in export production (assumed to equate to new production in a steady-state system; Laws, 1991) is smaller than originally estimated, such that an intensification of upwelling could feasibly explain this increase. In order to explain the increase of export production over this interval, an intensification of upwelling forced by easterly trade winds needs to be similar in size to that suggested for glacial periods in the Pleistocene (Janecek and Rea, 1985; Lyle and Baldauf, 2015). The higher trade winds could have also increased dust flux to this region, relaxing iron limitation for primary production. The apparent increase in biogenic silica over that of export production is expected during intervals of high productivity, both in production and preservation (Lyle and Baldauf, 2015). This would suggest a highly efficient biological pump with a high export ratio, more similar to a coastal upwelling system (Sarmiento and Gruber, 2006).

In order to test the feasibility of this mechanism, the increased productivity was simulated using a global carbon-cycle box model coupled to a sediment module (LOSCAR; Zeebe, 2012). Simulations demonstrate that these changes are not achievable without a concurrent increase in nutrient supply (modeled as PO_4^{3-}) to the surface Pacific. Increasing productivity causes an initial drop in pCO_2 (for details, see the Data Repository); however, this drop is limited because the productivity increase quickly (<1 k.y.) depletes the surface ocean of nutrients. Therefore, nutrient supply would have had to increase in order to maintain the elevated levels of export production in the BAR data. Modeling these types of changes in export production results in an increase in surface $\delta^{13}C$ by ~0.2‰; however, such a $\delta^{13}C$ rise would only be seen globally if the C was buried (and not simply remineralized at depth).

Intensification of upwelling could have contributed to this increase in nutrients, but we also suggest that development of North Atlantic Deep Water (NADW) at the time, due to tectonic forcing such as shoaling of the Central American Seaway or closing of the Tethys (e.g., Butzin et al., 2011; Zhang et al., 2011; Hamon et al., 2013, and references therein), may have played an important role in changing availability of nutrients in the water upwelling in the EEP. Development of NADW could have hindered upwelling of silica-rich Antarctic Bottom Water (AABW) in the North Atlantic (Cortese et al., 2004). These waters were instead rerouted to the Indo-Pacific (Cortese et al., 2004), thereby increasing nutrient concentrations, including silica, in the water upwelling in the EEP for an extended period of time. When silica becomes more available, diatoms can

[1]GSA Data Repository item 2016310, methods, Figures DR1–DR8, and Tables DR1 and DR2, is available online at www.geosociety.org/pubs/ft2016.htm, or on request from editing@geosociety.org.

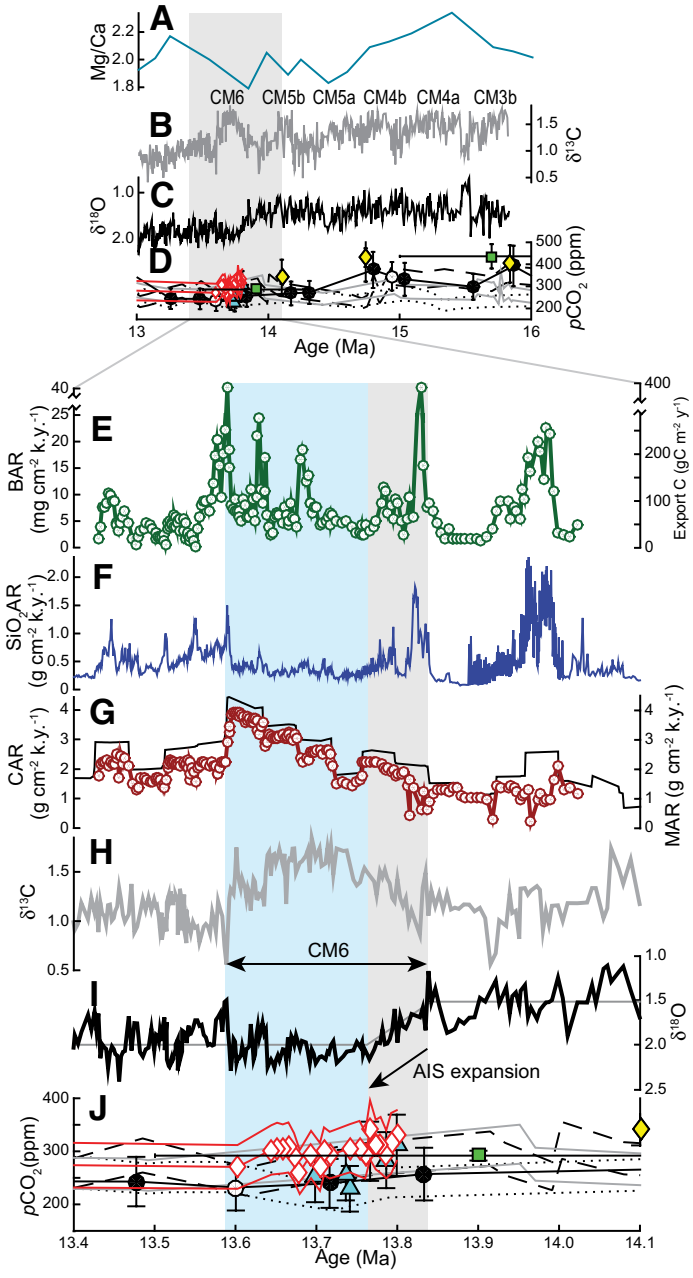

Figure 2. Middle Miocene paleoceanographic records. A: Benthic foraminifer Mg/Ca (Lear et al., 2015). B: Benthic foraminiferal $\delta^{13}C$ (Tian et al., 2013). C: Benthic foraminiferal $\delta^{18}O$ (Tian et al., 2013) with trends in the average values. D: Global records of atmospheric pCO_2 records from alkenone $\delta^{13}C$ from Ras il-Pellegrin (Malta) (red open diamonds and solid line with ±2 error envelopes; Badger et al., 2013), Ocean Drilling Program (ODP) Site 925 with propagated analytical uncertainties shown as error bars (yellow diamonds; Zhang et al., 2013), Deep Sea Drilling Project (DSDP) Site 588 (dotted black line), DSDP Site 608 (dashed black line), and ODP Site 730 (solid gray line) (Pagani et al., 1999); boron isotopes from the Ras il-Pellegrin section (blue filled triangles with propagated analytical uncertainties shown as error bars; Badger et al., 2013), and ODP Sites 761 (filled black circles) and 926 (open triangles) (Foster et al., 2012); and stomatal indices with propagated analytical uncertainties shown as error bars (green squares; Kürschner et al., 2008). The age models of Tian et al. (2013) (used in records A and B) and Pagani et al. (1999) have been shifted by –70 k.y. and –130 k.y., respectively, to match the age model by Holbourn et al. (2014), based on the positions of carbon maximum event 6 (CM6) in the records. E–J: Expanded views of A–D. E: Marine barite discrete measurements (this study). The y-axis on the right shows discrete BAR (barite mass accumulation rates) converted to export carbon using the relationship outlined in Eagle et al. (2003). F: SiO_2 accumulation rates (AR) from the X-ray fluorescence scanner (Shackford et al., 2014). G: $CaCO_3$ (CAR—$CaCO_3$ mass accumulation rates) measurements (open circles; this study) with mass accumulation rate (MAR) (black line; Tian et al., 2013). H: Benthic foraminiferal $\delta^{13}C$ (Tian et al., 2013). I: Benthic foraminiferal $\delta^{18}O$ (Tian et al., 2013) with trends in the average values. J: Global records of atmospheric pCO_2 (same as D). AIS—Antarctic Ice Sheet.

outcompete other primary producers such as coccolithophores, the dominant $CaCO_3$ producers in the modern EEP (Ragueneau et al., 2000). The availability of silica can control diatom production, and acts as a limiting nutrient in equatorial upwelling regions today (Dugdale and Wilkerson, 1998; Ragueneau et al., 2000). The formation of AABW also probably increased with increased glaciation of Antarctica (Cortese et al., 2004). Eventually (within 100 k.y.) this source of increased nutrients dissipated and/or trade winds and upwelling intensity decreased, returning export productivity to prior levels.

Given enough nutrients, these changes in productivity could draw down atmospheric pCO_2, causing global cooling, for which some evidence exists (Pagani et al., 1999; Lear et al., 2015; Fig. 2). It is possible that this interval of CO_2 drawdown preconditioned the climate system before the largest expansion of the AIS ca. 13.8 Ma, as suggested by Holbourn et al. (2014).

EXPORT PRODUCTION, CM6, AND AIS EXPANSION

Over the CM6 event, baseline values of BAR (average values not including peaks) are elevated (5.9 mg cm^{-2} $k.y.^{-1}$) compared to values outside the event (4.3 mg cm^{-2} $k.y.^{-1}$) that are comparable to present-day values. Because there is not a simultaneous increase in silica production, it is unlikely that export production is elevated due to an overall increase in primary productivity. Instead, elevated export production is probably caused by an increase in the particle export ratio, likely due to an increase in herbivore grazers, which would effectively increase the efficiency of the biological pump.

Peak BAR values as high as 40 mg cm^{-2} $k.y.^{-1}$ coincide with the beginning of CM6 and AIS expansion and are higher than all other currently investigated episodes of extreme Cenozoic climate change (Table DR1). These new data suggest that episodic variations occurred in EEP export production, indicating an extremely dynamic C cycle over the MMCT. Further work is needed to increase the resolution of the accumulation rate data (e.g., via extraterrestrial ^3He) in order to accurately quantify these abrupt changes and their possible contribution to atmospheric pCO_2 drawdown.

CONCLUSIONS

Overall, the MMCT was a time of elevated but variable export production in the EEP. The lack of Milankovitch cyclicity within the record of export production suggests that it is responding more to critical thresholds in the internal climate system, specifically nutrient supply via changes in ocean circulation (and upwelling), rather than being paced directly by orbital periodicity. This unique interval in Cenozoic climate history had atmospheric concentrations similar to today, but an extremely dynamic biological pump in the EEP that could have preconditioned the climate system before the largest expansion of the AIS and transition to a new, relatively stable glacial state. Additional proxy data from these and other cores are needed to reconstruct high-resolution dust flux, nutrient content, pCO_2, sea-surface and bottom-water temperatures (although care must be taken because sea-surface temperatures and production were generally decoupled during the Miocene in the EEP; e.g., Rousselle et al., 2013; Lear et al., 2015; Lyle and Baldauf, 2015), and other parameters to test these hypotheses linking ocean biogeochemistry and global climate during the MMCT.

ACKNOWLEDGMENTS

This research used samples provided by the Integrated Ocean Drilling Program and was supported by funds to Griffith from the University of Texas at Arlington. We thank Harry Rowe and Angela Lewis for access and assistance acquiring $CaCO_3$ mass accumulation rate data; Majie Fan and Arne Winguth for helpful discussions about the data; and Mitch Lyle, Kristina Faul, and two anonymous reviewers.

REFERENCES CITED

Badger, M.P.S., Lear, C.H., Pancost, R.D., Foster, G.L., Bailey, T.R., Leng, M.J., and Abels, H.A., 2013, CO_2 drawdown following the middle Miocene expansion of the Antarctic Ice Sheet: Paleoceanography, v. 28, p. 42–53, doi:10.1002/palo.20015.

Butzin, M., Lohmann, G., and Bickert, T., 2011, Miocene ocean circulation inferred from marine carbon cycle modeling combined with benthic isotope records: Paleoceanography, v. 26, PA1203, doi:10.1029/2009PA001901.

Chavez, F.P., and Barber, R.T., 1987, An estimate of new production in the equatorial Pacific: Deep-Sea Research, v. 34, p. 1229–1243, doi:10.1016/0198-0149(87)90073-2.

Cortese, G., Gersonde, R., Hillenbrand, C.D., and Kuhn, G., 2004, Opal sedimentation shifts in the world ocean over the last 15 Myr: Earth and Planetary Science Letters, v. 224, p. 509–527, doi:10.1016/j.epsl.2004.05.035.

Diester-Haass, L., Billups, K., Gröcke, D.R., François, L., Lefebvre, V., and Emeis, K.C., 2009, Mid-Miocene paleoproductivity in the Atlantic Ocean and implications for the global carbon cycle: Paleoceanography, v. 24, PA1209, doi:10.1029/2008PA001605.

Dugdale, R.C., and Wilkerson, F.P., 1998, Silicate regulation of new production in the equatorial Pacific upwelling: Nature, v. 391, p. 270–273, doi:10.1038/34630.

Eagle, M., Paytan, A., Arrigo, K.R., van Dijken, G., and Murray, R.W., 2003, A comparison between excess barium and barite as indicators of carbon export: Paleoceanography, v. 18, 1021, doi:10.1029/2002PA000793.

Foster, G.L., Lear, C.H., and Rae, J.W.B., 2012, The evolution of pCO_2, ice volume and climate during the middle Miocene: Earth and Planetary Science Letters, v. 341–344, p. 243–254, doi:10.1016/j.epsl.2012.06.007.

Griffith, E.M., Calhoun, M., Thomas, E., Averyt, K., Erhardt, A., Bralower, T., Lyle, M., Olivarez-Lyle, A., and Paytan, A., 2010, Export productivity and carbonate accumulation in the Pacific Basin at the transition from a greenhouse to icehouse climate (late Eocene to early Oligocene): Paleoceanography, v. 25, PA3212, doi:10.1029/2010PA001932.

Hamon, N., Sepulchre, P., Lefebvre, V., and Ramstein, G., 2013, The role of eastern Tethys seaway closure in the Middle Miocene Climatic Transition (ca. 14 Ma): Climate of the Past, v. 9, p. 2687–2702, doi:10.5194/cp-9-2687-2013.

Holbourn, A., Kuhnt, W., Schulz, M., Flores, J., and Andersen, N., 2007, Orbitally-paced climate evolution during the middle Miocene "Monterey" carbon-isotope excursion: Earth and Planetary Science Letters, v. 261, p. 534–550, doi:10.1016/j.epsl.2007.07.026.

Holbourn, A., Kuhnt, W., Lyle, M., Schneider, L., Romero, O., and Andersen, N., 2014, Middle Miocene climate cooling linked to intensification of eastern equatorial Pacific upwelling: Geology, v. 42, p. 19–22, doi:10.1130/G34890.1.

Janecek, T.R., and Rea, D.K., 1985, Quaternary fluctuations in the Northern Hemisphere trade winds and westerlies: Quaternary Research, v. 24, p. 150–163, doi:10.1016/0033-5894(85)90002-X.

Kender, S., Yu, J., and Peck, V.L., 2014, Deep ocean carbonate ion increase during mid Miocene CO_2 decline: Scientific Reports, v. 4, 4187, doi:10.1038/srep04187.

Kürschner, W.M., Kvaček, Z., and Dilcher, D.L., 2008, The impact of Miocene atmospheric carbon dioxide fluctuations on climate and the evolution of terrestrial ecosystems: National Academy of Sciences Proceedings, v. 105, p. 449–453, doi:10.1073/pnas.0708588105.

Laws, E.A., 1991, Photosynthetic quotients, new production, and net production, and net community production in the open ocean: Deep-Sea Research, v. 38, p. 143–167, doi:10.1016/0198-0149(91)90059-O.

Lear, C.H., Coxall, H.K., Foster, G.L., Lunt, D.J., Mawbey, E.M., Rosenthal, Y., Sosdian, S.M., Thomas, E., and Wilson, P.A., 2015, Neogene ice volume and ocean temperatures: Insights from infaunal foraminiferal Mg/Ca paleothermometry: Paleoceanography, v. 30, p. 1437–1454, doi:10.1002/2015PA002833.

Lyle, M., and Baldauf, J., 2015, Biogenic sediment regimes in the Neogene equatorial Pacific, IODP Site U1338: Burial, production, and diatom community: Palaeogeography, Palaeoclimatology, Palaeoecology, v. 433, p. 106–128, doi:10.1016/j.palaeo.2015.04.001.

Martin, J.H., et al., 1994, Testing the iron hypothesis in ecosystems of the equatorial Pacific Ocean: Nature, v. 371, p. 123–129, doi:10.1038/371123a0.

Pagani, M., Arthur, M.A., and Freeman, K.H., 1999, Miocene evolution of atmospheric carbon dioxide: Paleoceanography, v. 14, p. 273–292, doi:10.1029/1999PA900006.

Pälike, H., Lyle, M., Nishi, H., Raffi, I., Gamage, K., Klaus, A., and the Expedition 320/321 Scientists, 2010, Pacific equatorial age transect: Proceedings of the Integrated Ocean Drilling Program Expedition 320/321: Tokyo, Integrated Ocean Drilling Program Management International, Inc., http://publications.iodp.org/proceedings/320_321/32021toc.htm.

Paytan, A., and Griffith, E., 2007, Marine barite: Recorder of variations in ocean export productivity: Deep-Sea Research. Part II, Topical Studies in Oceanography, v. 54, p. 687–705, doi:10.1016/j.dsr2.2007.01.007.

Paytan, A., Kastner, M., and Chavez, F.P., 1996, Glacial to interglacial fluctuations in productivity in the equatorial Pacific as indicated by marine barite: Science, v. 274, p. 1355–1357, doi:10.1126/science.274.5291.1355.

Ragueneau, O., et al., 2000, A review of the Si cycle in the modern ocean: Recent progress and missing gaps in the application of biogenic opal as a paleoproductivity proxy: Global and Planetary Change, v. 26, p. 317–365, doi:10.1016/S0921-8181(00)00052-7.

Rousselle, G., Beltran, C., Sicre, M.A., Raffi, I., and De Rafélis, M., 2013, Changes in sea-surface conditions in the Equatorial Pacific during the middle Miocene–Pliocene as inferred from coccolith geochemistry: Earth and Planetary Science Letters, v. 361, p. 412–421, doi:10.1016/j.epsl.2012.11.003.

Sarmiento, J.L., and Gruber, N., 2006, Ocean biogeochemical dynamics: New Jersey, Princeton University Press, 528 p.

Shackford, J.K., Lyle, M., Wilkens, R., and Tian, J., 2014, Data report: Raw and normalized elemental data along the Site U1335, U1336, and U1337 splices from X-ray fluorescence scanning, *in* Pälike, H., et al., Proceedings of the Integrated Ocean Drilling Program 320/321: Tokyo, Integrated Ocean Drilling Program Management International, Inc., doi:10.2204/iodp.proc.320321.216.2014.

Shevenell, A.E., Kennett, J.P., and Lea, D.W., 2008, Middle Miocene ice sheet dynamics, deep-sea temperatures, and carbon cycling: A southern ocean perspective: Geochemistry, Geophysics, Geosystems, v. 9, Q02006, doi:10.1029/2007GC001736.

Sigman, S.M., and Boyle, E.A., 2000, Glacial/interglacial variations in atmospheric carbon dioxide: Nature, v. 407, p. 859–869, doi:10.1038/35038000.

Tian, J., Yang, M., Lyle, M.W., Wilkens, R., and Shackford, J.K., 2013, Obliquity and long eccentricity pacing of the middle Miocene climate transition: Geochemistry, Geophysics, Geosystems, v. 14, p. 1740–1755, doi:10.1002/ggge.20108.

Vincent, E., and Berger, W.H., 1985, Carbon dioxide and polar cooling in the Miocene: The Monterey Hypothesis, *in* Sundquist, E.T. and Broecker, W.S., eds., The carbon cycle and atmospheric CO_2: Natural variations Archean to present: American Geophysical Union Geophysical Monograph 32, p. 455–468, doi:10.1029/GM032p0455.

Woodruff, F., and Savin, S., 1991, Mid-Miocene isotope stratigraphy in the deep sea: High-resolution correlations, paleoclimatic cycles, and sediment preservation: Paleoceanography, v. 6, p. 755–806, doi:10.1029/91PA02561.

Zachos, J.C., Pagani, M., Sloan, L.C., Thomas, E., and Billups, K., 2001, Trends, rhythms, and aberrations in global climate 65 Ma to present: Science, v. 292, p. 686–693, doi:10.1126/science.1059412.

Zeebe, R.E., 2012, LOSCAR: Long-term Ocean-atmosphere-Sediment CArbon cycle Reservoir Model v2.0.4: Geoscientific Model Development, v. 5, p. 149–166, doi:10.5194/gmd-5-149-2012.

Zhang, Y.G., Pagani, M., Liu, Z.H., Bohaty, S.M., and DeConto, R., 2013, A 40-million-year history of atmospheric CO_2: Royal Society of London Philosophical Transactions, ser. A, v. 371, p. 1–20, doi:10.1098/rsta.2013.0096.

Zhang, Z., Nisancioglu, K.H., Flatøy, F., Bentsen, M., Bethke, I., and Wang, H., 2011, Tropical seaways played a more important role than high latitude seaways in Cenozoic cooling: Climate of the Past, v. 7, p. 801–813, doi:10.5194/cp-7-801-2011.

Manuscript received 24 June 2016
Revised manuscript received 27 August 2016
Manuscript accepted 29 August 2016

Printed in USA